 MCB, vol.14, no.1, pp. 19-31, 2017

Anatomical Variations in Circle of Willis and Intracranial Aneurysm Formation

Zhen Liu[1], Yan Cai[1], Guo-Zhong Chen[2], Guang-Ming Lu, Zhi-Yong Li[1,3*]

Abstract: Intracranial aneurysm (IA) can be commonly found in the circle of Willis (Cow), and a higher morbidity of IA is found to be associated with a higher percentage of an incomplete Cow. Hemodynamic factors are believed to play an important role in aneurysm formation. However, how the anatomical variations in Cow leads to hemodynamic difference and what hemodynamic parameters play important roles in aneurysm formation have not been quantified and assessed. Thirty patients were included and based one computed tomography angiography, they were divided into three groups (10 patients per group): a normal group (normal Cow and without aneurysms), an absence group (lacking the anterior cerebral artery and with aneurysms), and a hypoplasia group (hypoplasia of the anterior cerebral artery and with aneurysms). Patient-specific 3D models of the Cow were reconstructed by removing all the aneurysms and CFD simulations were performed on the 30 patient-specific models. Six hemodynamic parameters (blood pressure, average wall shear stress (AWSS), AWSS gradient (AWSSG), oscillatory shear index (OSI), aneurysm formation indicator (AFI), and gradient oscillatory number (GON)) were analyzed and compared between the three groups. The hypoplasia group was found to be significantly higher in AWSS (7.41 ± 1.70vs5.44 ± 1.31, $p=0.029$) and AFI (0.9959 ± 0.0012vs0.9945 ± 0.0011, $p=0.037$) than those of the normal group. To conclude, anatomical variation in the anterior circulation of Cow resulted in abnormal hemodynamic environment of cerebral arteries, and this may lead to formation of intracranial aneurysm. AWSS and changes in the direction of WSS may be the important hemodynamic parameters leading to aneurysm formation.

[1]School of Biological Science and Medical Engineering, Southeast University, Nanjing 210096, China.

[2] Department of Medical Imaging, Jinling Hospital, Medical School of Nanjing University, Nanjing, Jiangsu, 210002, China.

[3] School of Chemistry, Physics and Mechanical Engineering, Queensland University of Technology, Brisbane, QLD 4001, Australia.

*Corresponding author: Zhi-Yong Li

School of Biological Science and Medical Engineering,Southeast University,Nanjing 210096, China.

Tel & Fax: +86 25 83792620Email: 101011308@seu.edu.cn

Keywords: Intracranial aneurysm, circle of Willis, hemodynamic, anatomical variation, wall shear stress.

1 Background

Intracranial aneurysm (IA) is the main precursor of subarachnoid hemorrhage [Humphrey and Taylor (2008)]. The prevalence of IA in a population ranges from 3.6%–6%, and 1%–2% of IAs rupture every year. Considering the high disability and mortality rate, the social and economic impact is enormous. IA is a type of cerebral vascular disease associated with deficiencies in the arterial wall. It often occurs around bifurcations at the circle of Willis (Cow) [Sadasivan, Fiorella and Woo, et al. (2013)]. Cow is a major collateral circulation that has an important role in maintaining adequate blood flow and balancing perfusion blood pressure [Li, Li and Lv, et al. (2011); Liebeskind (2003)]. Hence, the structure, anatomical variations, and the degree of openness of the Cow may affect the compensatory function, which can lead to cerebrovascular disease [Ingebrigtsen, Morgan, Faulder, et al. (2004)]. IAs arise predominantly along or within the vicinity of the Cow, with over 85% of IAs occurring in the anterior part of the Cow[Tanweer, Wilson and Metaxa, et al. (2014)]. However, more than 50% of the general population has an incomplete Cow[Alpers, Berry and Paddison (1959); Moore, David and Chase, et al. (2006)]. Previous studies have suggested that anomalies in the geometry of the Cow, such as hypoplasia and absence, occur more frequently in patients with aneurysms than in controls[Sadasivan, Fiorella and Woo, et al. (2013); Kayembe, Sasahara and Hazama (1984); Bor, Velthuis and Majoie, et al. (2008)].

Hemodynamics may be one of the most important factors related to the growth, development, and rupture of aneurysms. The formation of IA is thought to be caused by remodeling of the arterial wall under long-term and complicated hemodynamic environment [Le, Zhu and Li, et al. (2013); Chien, Castro and Tateshima, et al. (2009); Norman and Powell (2010)]. However, it remains controversial as to whether high or low WSS leads to IA initiation, growth and rupture [Meng, Tutino and Xiang, et al. (2014)]. Previous studies have shown that high wall shear stress (WSS) can modify the expression of vascular endothelial cells (VEC), then further affect cells proliferation and migration [Chiu, Chen and Lee, et al. (2003); Blackman, Thibault and Barbee (2000); Zhao, Chen and Miao, et al. (2002)]. These VEC studies have been the basis of discussing pathogenesis of aneurysms. However, it is argued that VEC have anomalous response to WSS and the anomalous temporal and spatial gradients of WSS which may contribute to an unstable progressive degradation of the arterial wall and the formation of the aneurysm [Lasheras (2007)]. Thus, further study on the local hemodynamic environment in patient-specific cases is essential to have an improved understanding of the mechanism of IA formation. The hemodynamic parameters are dependent of the local arterial geometries of the Cow. Therefore, there is a great need to further investigate the current common anatomical variations in Cow and the local flow dynamics in order to evaluate which hemodynamic parameters play an important role and how much difference of the hemodynamic parameters between different patient groups.

The purpose of this study is to quantify the local hemodynamic parameters in patients

with normal and abnormal Cows, and evaluate the impact of different anatomical variations in Cow on the morbidity of intracranial aneurysms. Thirty patients were recruited in this study and their patient-specific 3D models were reconstructed after removing the aneurysms. Using computational fluid dynamics (CFD), different hemodynamic factors were assessed and compared between the patients.

2 Methods

2.1 Patients

Thirty patients were recruited at the Department of Radiology in Nanjing General Hospital. Patients' ages ranged from 24 to 80 years with a median age of 51.5 years. 17 were male and 13 were female. Computed tomography angiography (CTA) was performed to evaluate the CoWs and detect the IAs. The patients were divided into three groups (10 patients per group): a normal group (normal CoW and without aneurysms), an absence group (lacking the anterior cerebral artery and with aneurysms), and a hypoplasia group (hypoplasia of the anterior cerebral artery and with aneurysms). Patient information for each group is shown in Table 1. This study was approved by the internal review board and informed written consent was obtained.

Table 1: Patient information

	Sex		Age
Group	Male	Female	(ave/years)
Normal	7	3	46.7
Absence	4	6	54.7
Hypoplasia	6	4	53.1
Total	17	13	51.5

2.2 Patient-specific 3D model reconstruction

The imaging data in DICOM format were imported into ScanIP (Version 6.0, Simpleware Ltd.) for image segmentation and 3D reconstruction based on our established protocol [Ren, Chen and Li (2015); Ren, Chen and Liu, et al. (2016)]. First, the surface boundaries of the cerebral arteries were identified through adjusting the threshold value, and a rough Cow model was built. Then, using crop and floodfill functions, the extraneous arteries and regions were removed from the model. In particular, posterior cerebral circulation has only a minor impact on anterior circulation. Bilateral posterior cerebral arteries were also removed from the Cow region in all models because anterior circulation was the main focus. Finally, the model was modified through 3D editing processing (smooth, dilate, and erode) and then converted to a patient-specific 3D model. Our laboratory has extensive experience in the patient-specific arterial model development [Ren, Chen and Liu, et al. (2016)].

All patients in the two abnormal Cow groups had anterior communicating artery (Acoma) aneurysms. Inorderto study the formation of aneurysms, the hypothetical pre-aneurysmal vascular model was reconstructed. The reconstruction of pre-aneurysmal vascular was achieved by removing the aneurysms using the 3D editing function in simpleware. The

specific editing area is shown in Fig. 1. Thirty patient-specific 3D models were reconstructed based on different anatomical variation in the anterior circulation of Cow. Fig. 2 shows an example of the Cow model for each group.

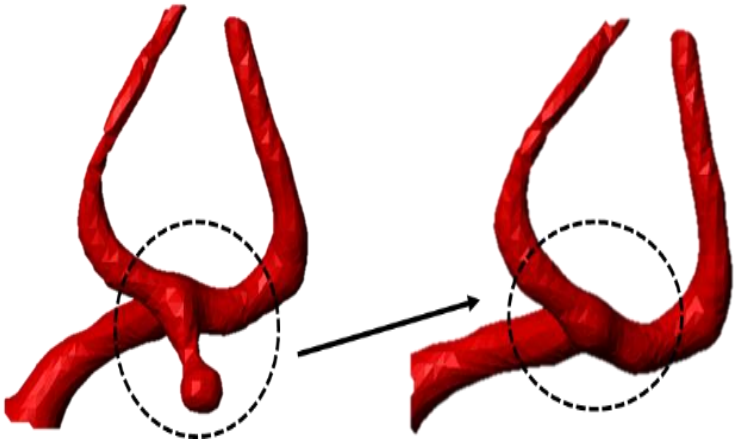

Figure 1: 3D reconstruction of the arterial model with and without an aneurysm.

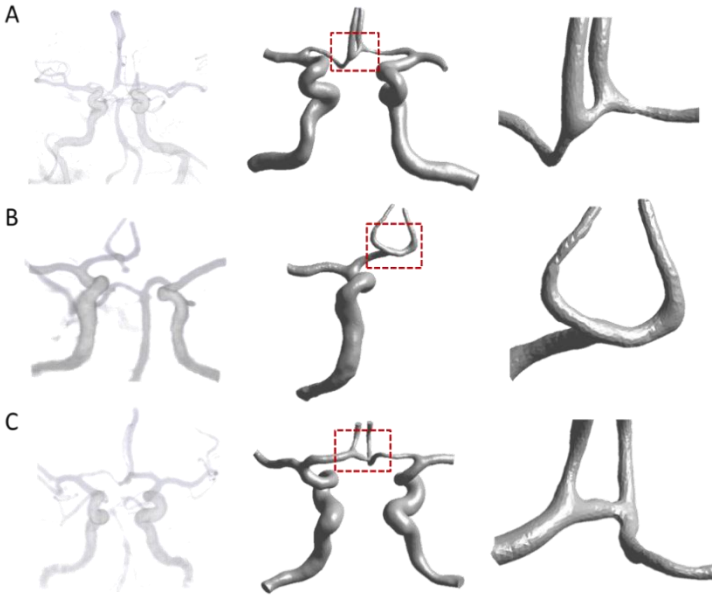

Figure 2: Examples of the CoW model from each patient group. A: the normal group. B: the absence group. C: the hypoplasia group.

2.3 CFD simulation

CFD analyses were performed to investigate the hemodynamic environment of the Cow models. All 3D models were imported into Workbench Mesh, Version 15.0 (ANSYS Inc.), and an unstructured tetrahedral mesh with refinement mesh in Acoma region and thinner

arteries was generated for the fluid domain.

Blood flow was simulated on the basis of the unsteady Navier-Strokes equations using a finite volume formulation with Fluent, Version 15.0 (ANSYS Inc.). Blood was assumed to be a Newtonian fluid with constant density $\rho = 1056\,\mathrm{kg/m^3}$ and viscosity $\mu = 0.0035\,\mathrm{Pa.s}$. Arterial vessels were modeled as a rigid wall with no-slip boundary condition. Based on phase contrast MRI, a pulsatile volume flow waveform of a healthy volunteer in the ICA (Fig. 3) was used to transform into blood velocity at the inlet section according to the volume flow rate. Pulsatile velocity (inlet) and constant pressure (outlet) were set as boundary conditions [Ford, Alperin and Lee, et al. (2005); Alnaes, Isaksen and Mardal, et al. (2007)]. Bilateral anterior cerebral arteries and middle cerebral arteries served as simulation outlets and bilateral internal carotid arteries as inlets. In the simulation, the convergence criterion was satisfied when the residual of continuity and the velocity component was less than 10^{-4}.

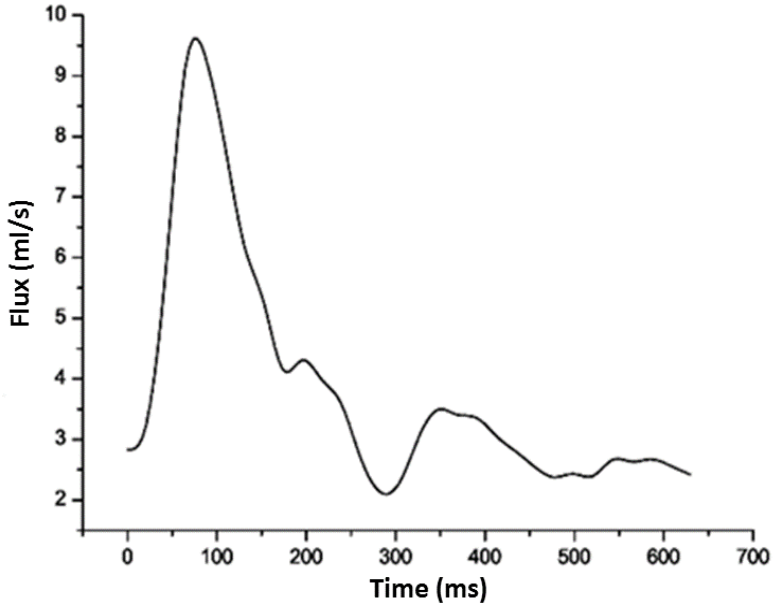

Figure 3: The pulsatile flow waveform used as the flow boundary condition at the inlet.

2.4 Hemodynamic parameters

The following six hemodynamic parameters were investigated [Chen, Selimovic and Thompson et al. (2013)]: blood pressure, average wall shear stress (AWSS), average wall shear stress gradient (AWSSG), oscillatory shear index (OSI), aneurysm formation indicator (AFI), and gradient oscillatory number (GON).

As reported by Cheng et al, the WSS vector t_s is defined as follows [Cheng, Parker and Taylor (2002)]:

$$t_s = \mathrm{t} - (\mathrm{t}\cdot\mathrm{n})\mathrm{n} \quad (1)$$

Here, n is the inward unit vector at any point on the lumen surface. The traction force vectors at the same point are defined as $\mathrm{t} = \sigma\mathrm{n}$, where σ is the fluid stress tensor.

Then the magnitude of t_s can be denoted as $\tau(t)$ and its time-averaged value as AWSS can be calculated as follows:

$$\text{AWSS} \equiv \tau_{av} = \frac{1}{T}\int_0^T \tau dt \tag{2}$$

In a similar method, the tangential component of WSSG vector on the vessel surface is defined as follows:

$$g_s = \nabla\tau - (\nabla\tau \cdot \text{n})\text{n} \tag{3}$$

The time-averaged WSSG is calculated as follows:

$$\text{AWSSG} = \frac{1}{T}\int_0^T |g_s| dt \tag{4}$$

In a cardiac cycle, the OSI [He and Ku (1996)] is computed as follows:

$$\text{OSI} = \frac{1}{2}\left\{1 - \frac{\frac{1}{T}\int_0^T t_s dt}{\tau_{av}}\right\} \tag{5}$$

AFI has been proposed to quantify WSS changes in direction [Mantha, Karmonik and Benndorf et al. (2006)]. AFI is the cosine of the angle $[\cos(\theta)]$ between the instantaneous WSS vector and the time-averaged WSS vector.

$$\text{AFI} = \frac{t_s \cdot \overline{\frac{1}{T}\int_0^T t_s dt}}{\tau \cdot |\overline{\frac{1}{T}\int_0^T t_s dt}|} \tag{6}$$

Because AFI is an instantaneous quantity, the minimum value of AFI during the cardiac cycle (t=0.1256s) can be selected and calculated.

GON is defined as follows [Shimogonya, Ishikawa and Imai et al. (2009)] :

$$\begin{cases} \text{GON} = 1 - \dfrac{|\int_0^T G dt|}{\int_0^T |G| dt} \\ \text{G} = \left(\dfrac{\partial t_{sp}}{\partial p}, \dfrac{\partial t_{sq}}{\partial q}\right) \end{cases} \tag{7}$$

Here, t_{sp} is a component of t_s resolved in the direction of the mean WSS vector, and t_{sq} is the (in-plane) component of t_s resolved in the direction perpendicular to the mean WSS vector. GON is computed to quantify the degree of oscillating tension/compression forces.

3 Statistical analysis

The differences of the above hemodynamic parameters between the normal group and each of the abnormal groups were analyzed using an independent sample T test. *P* value <0.05 was regarded as statistically significance, and all tests were 2-sided. Statistical analyses were performed using SPSS19 (SPSS Inc. Chicago, Ill).

4 Results

The hemodynamic parameters were analyzed and compared between the three patient groups. An example of the computed contours of the hemodynamic parameters of a patient from each group are shown in Fig. 4, where A – F is AWSS, AWSSG, OSI, AFI, GON, and pressure. The black arrow indicates the site of the aneurysm.

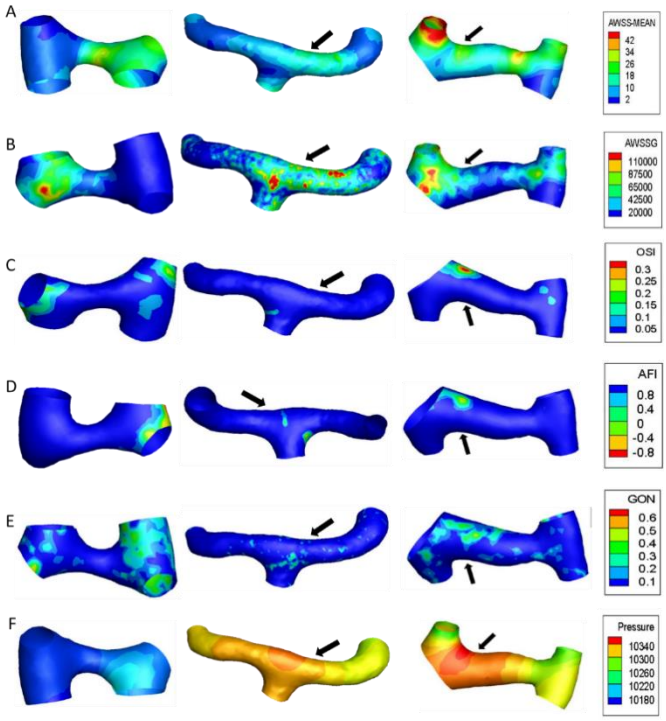

Figure 4: The computed contour maps of the hemodynamic parameters between the normal group (left), the absence group (middle) and the hypoplasia group (right). A: AWSS. B: AWSSG. C: OSI. D: AFI. E, GON. F: pressure. (Black arrow: the site of aneurysm).

As shown in Fig. 4, almost all the variations in the hemodynamic parameters occurred in the anterior communicating artery and the bifurcation, origins of branching. These regions had higher degree of curvature, where the flow was more complicated with a larger variation during the pulsatile cardiac cycle [Lasheras (2007)]. The AWSS, AWSSG and pressure were larger in the two patient groups with abnormal Cows than those of the normal group. Moreover, the three parameters had wider high-value areas at the anterior communicating artery, where the aneurysms were found. A similar pattern has also been shown in previous reports [Lasheras (2007); Nerem, Harrison and Taylor, et al. (1993)]. As for OSI, AFI, and GON, the computed contours showed similar levels of regularity between the three groups.

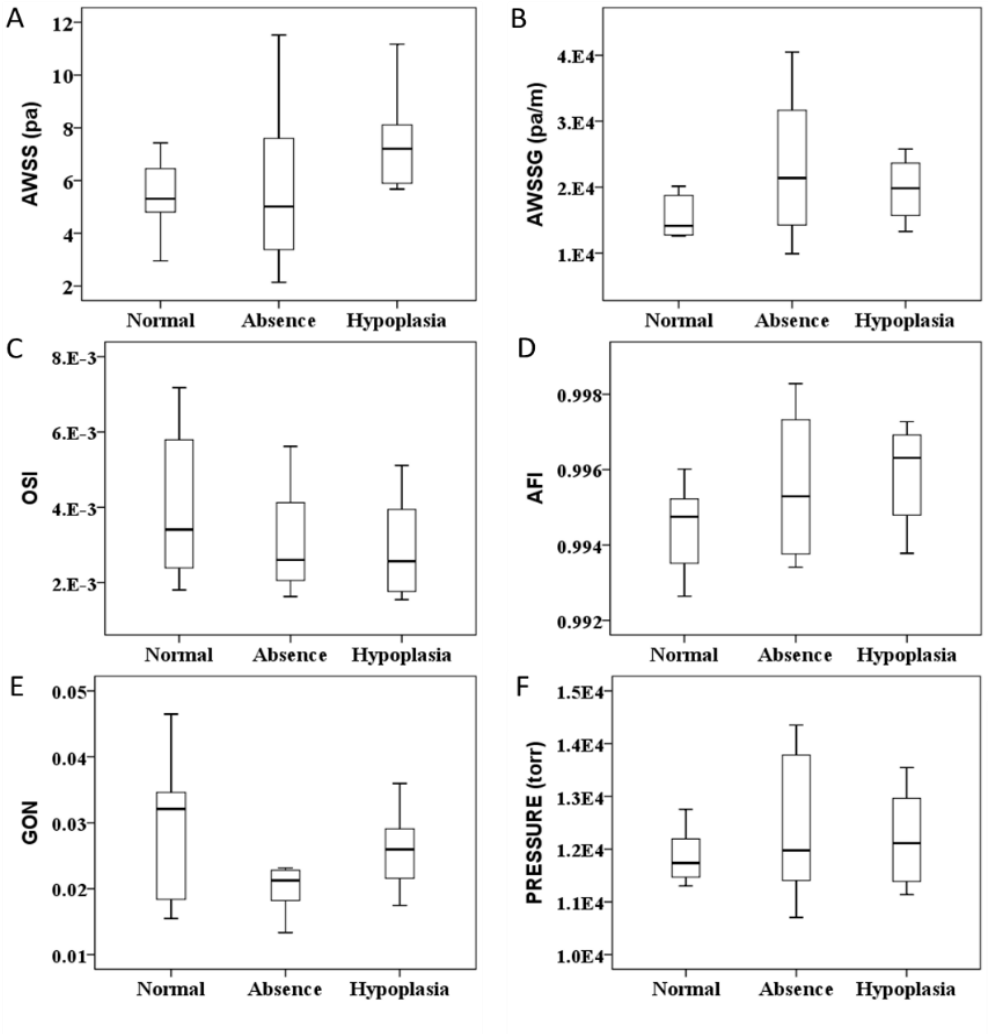

Figure 5: Boxplot of the computed hemodynamic parameters. A: AWSS. B: AWSSG. C: OSI. D: AFI. E: GON. F: pressure.

Fig. 5 is the boxplot of the six hemodynamic parameters. AWSS, AWSSG, AFI, and pressure had higher maximum values in both the absence group and the hypoplasia group than those in the normal group. In contrast, the other two parameters, OSI and GON, were lower in the two abnormal groups. Table 2 outlines the average hemodynamic parameters of the three groups. Similarly, the two abnormal groups had much larger values in AWSS, AWSSG and pressure. This is consistent with the contour and boxplot illustrated above.

Table 2: The computed results of the hemodynamic parameters of the three patient groups.

	Normal	Absence	Hypoplasia
AWSS	5.44 ±1.31	5.71 ±2.95	7.41 ±1.70
AWSSG	1.55 ±0.30e+4	2.31 ±1.03e+4	1.97 ±0.44e+4
OSI	0.0040 ±0.0020	0.0031 ±0.0014	0.0029 ±0.0013
AFI	0.9945 ±0.0011	0.9956 ±0.0018	0.9959 ±0.0012
GON	0.029 ±0.010	0.020 ±0.003	0.026 ±0.006
Pressure	1.19 ±0.05e+4	1.24 ±0.13e+4	1.22 ±0.09e+4

Six hemodynamic parameters were analyzed using an independent sample T-test. Table 3 is the specific *p* value of six parameters. The statistical results suggest that there is no significant difference between the normal group and the absence group. However, the hypoplasia group was found to be significantly higher in AWSS (7.41 ±1.70 vs 5.44 ±1.31, p=0.029) and AFI (0.9959 ±0.0012 vs 0.9945 ±0.0011, p=0.037) than those of the normal group.

Table 3: *P* value of independent sample T test

	AWSS	AWSSG	OSI	AFI	GON	Pressure
Normal—Absence	0.829	0.095	0.332	0.186	0.055	0.302
Normal—Hypoplasia	0.029	0.057	0.229	0.037	0.474	0.379

5 Discussion

In this study, patient-specific 3D computational biomechanical models and numerical simulations were developed. The associations between the geometrical variations in the Cow and the hemodynamic parameters were quantitatively evaluated and compared between the three patient groups. The study demonstrated a difference in the hemodynamic parameters between the patients with normal and abnormal Cows. The difference in hemodynamics may be associated with the likelihood of the formation of an IA in patients with abnormal Cows, such as hypoplasia and absence groups, and provide some insights to why an aneurysm occurs more frequently in the incomplete Cow patients as found in clinical practice [Kayembe, Sasahara and Hazama (1984)].

The hemodynamic factors have been studied and recognized by increasing numbers of researchers. Hemodynamic variables such as WSS and the WSS gradient have been associated with the formation of aneurysms [Lasheras (2007); Boussel, Rayz and Martin, et al. (2008)]. One generally accepted hypothesis states that mechanical degeneration of the bifurcation takes place because of the high shear stress. Some other researchers believe that the high shear stress gradient is related to the initiation of aneurysms[Lasheras (2007)].

Oscillatory shear stress due to pulsatile flow has also been investigated to correlate with aneurysm formation [Sadasivan, Fiorella and Woo, et al. (2013)]. It was also proposed that AFI may be a suitable indicator of the instantaneous effect of WSS fluctuations on endothelial cells [Mantha, Karmonik and Benndorf, et al. (2006)]. Moreover, GON is a function of WSSG, and it can represent tension/compression forces acting on endothelial cells [Shimogonya, Ishikawa and Imai, et al. (2009)]. These two parameters have been proposed in recent years. The AFI represents changes in WSS at a certain instance, and GON represents fluctuation of WSSG during a cardiac cycle [Shimogonya, Ishikawa and Imai, et al. (2009)]. The changes in AFI and GON values were found to coincide with the locations of aneurysm formation. In this study, we have investigated all the six hemodynamic parameters and evaluate which parameters are more suitable indicators of the hemodynamic environment of CoW and which parameters are more sensible to the geometrical variations.

The hemodynamic contours between the patients with normal and two abnormal Cows show that there are visible changes in the hemodynamic parameters at the Acoma and the bifurcation areas. A high AWSS distribution was observed at the anterior communicating artery, bifurcation and branch of arteries. This is due to the high curvature and complex geometry in these areas, which can influence the blood flow under the unsteady pulsatile condition [Nixon, Gunel and Sumpio (2010); Gibbons and Dzau (1994)] . An increase in blood flow velocity results in an increase in WSS at area of stenosis [Nerem, Harrison and Taylor, et al. (1993)]. In a similar way, the high AWSSG in this region also corresponds to a large spatial difference in WSS. High WSS and WSSG indicate that there may be more impinging blood flow acting on the vessel wall [Lasheras (2007)]. When blood flow is disturbed, WSS is also disturbed, leading to a variation in the WSS along the adjacent wall. From this study, the patient group with lacking the anterior artery showed higher AWSS, AWSSG and blood pressure distributions than the normal group. It has an impact on the inner layer of the arterial walls, especially at the anterior communicating artery and branch area. The formation of the cerebral aneurysm may be the result of the hemodynamic impact at these regions in the CoW. However, future clinical studies and follow up data are needed to future validate the current computational study.

6 Conclusion

The patients with anatomical variations of Cow showed a higher AWSS value and a larger region of variation than those with normal Cows. Anatomical variation in the anterior circulation of Cow resulted in abnormal hemodynamic environment of cerebral arteries, and this may lead to formation of intracranial aneurysm. Hypoplasia of the anterior cerebral artery may tend to have a higher possibility of aneurysm formation. Average wall shear stress (WSS) and changes in the direction of WSS may be the important hemodynamic parameters leading to aneurysm formation.

Source of Funding: This study was partially supported by the National 973 Basic Research Program of China [No. 2013CB733800], the National Natural Science Foundation of China (NSFC) (No. 11272091, 11422222, 31470043, 11772093), and ARC (FT140101152).

References

Alnaes, M.S.; Isaksen, J.; Mardal, K.A.;Romner, B.; Morgan, M.K.; Ingebrigtsen, T. (2007): Computation of hemodynamics in the circle of Willis. *Stroke; a journal of cerebral circulation*, vol.38, no.9, pp.:2500-2505.

Alpers, B.J.; Berry, R.G.; Paddison, R. M.(1959): Anatomical studies of the circle of Willis in normal brain. *A.M.A. archives of neurology and psychiatry,* vol.81, no.4, pp. 409-418.

Blackman, B.R.; Thibault, L.E.; Barbee, K.A. (2000): Selective modulation of endothelial cell [Ca2+]i response to flow by the onset rate of shear stress. *Journal of biomechanical engineering*, vol.122, no.3, pp.274-282.

Bor, A.S.; Velthuis, B.K.; Majoie, C.B.; &Rinkel, G.J. (2008): Configuration of intracranial arteries and development of aneurysms: a follow-up study. *Neurology*, vol.70, no.9, pp.700-705.

Boussel, L.; Rayz, V.C.; Martin, A.; Acevedo-Bolton, G.; Lawton, M.; Higashida, R.; Smith, W.; Young, W.; Saloner, D. (2008): Aneurysm growth occurs at region of low wall shear stress: patient-specific correlation of hemodynamics and growth in a longitudinal study. *Stroke; a journal of cerebral circulation*,vol.39, no.39, pp.2997-3002.

Chen, H.; Selimovic, A.; Thompson, H.; Chiarini, A.; Penrose, J.; Ventikos, Y.; Watton, P.N.(2013): Investigating the influence of haemodynamic stimuli on intracranial aneurysm inception. *Annals of biomedical engineering*,vol.41, no.7, pp.1492-1504.

Cheng, C.P.; Parker, D.; Taylor, C.A. (2002): Quantification of wall shear stress in large blood vessels using Lagrangian interpolation functions with cine phase-contrast magnetic resonance imaging. *Annals of biomedical engineering,* vol.30, no.8, pp.1020-1032.

Chien, A.; Castro, M.A.; Tateshima, S.; Sayre, J.; Cebral, J.; Vinuela, F. (2009): Quantitative hemodynamic analysis of brain aneurysms at different locations. *AJNR. American journal of neuroradiology,*vol.30, no.8, pp.1507-1512.

Chiu, J.J.; Chen, L.J.; Lee, P.L.; Lee, C.I.; Lo, L.W.; Usami, S.; Chien, S. (2003): Shear stress inhibits adhesion molecule expression in vascular endothelial cells induced by coculture with smooth muscle cells. *Blood*,vol.101, no.7, pp.2667-2674.

Ford, M.D.; Alperin, N.; Lee, S.H.; Holdsworth, D.W.; Steinman, D.A. (2005): Characterization of volumetric flow rate waveforms in the normal internal carotid and vertebral arteries. *Physiological measurement*,vol.26, no.4, pp.477-488.

Gibbons, G.H.; Dzau, V.J. (1994): The emerging concept of vascular remodeling. *New England Journal of Medicine*,vol.330, no.330, pp.1431-1438.

He, X; Ku, DN. (1996): Pulsatile flow in the human left coronary artery bifurcation: average conditions. *Journal of biomechanical engineering*,vol.118, no.1, pp.74-82.

Humphrey, J. D.; Taylor, C. A. (2008): Intracranial and abdominal aortic aneurysms: similarities, differences, and need for a new class of computational models. *Annual review of biomedical engineering*,pp.10:221-246.

Ingebrigtsen, T.; Morgan, M.K.; Faulder, K.; Ingebrigtsen, L.; Sparr, T.; Schirmer, H. (2004): Bifurcation geometry and the presence of cerebral artery aneurysms. *Journal of neurosurgery*,vol.101, no.1, pp.108-113.

Kayembe, K.N.; Sasahara, M.; Hazama, F.(1984): Cerebral aneurysms and variations in the

circle of Willis. *Stroke; a journal of cerebral circulation,*vol.15, no.5, pp.846-850.

Lasheras, J.C. (2007):The Biomechanics of Arterial Aneurysms. *Annual Review of Fluid Mechanics,*vol.39, no.1, pp.293-319.

Le, W.J.; Zhu, Y.Q.; Li, M.H.; Yan, L.; Tan, H.Q.; Xiao, S.M.; Cheng, Y.S. (2013): New method for retrospective study of hemodynamic changes before and after aneurysm formation in patients with ruptured or unruptured aneurysms. *BMC neurology,*pp.13:166.

Liebeskind, D. S. (2003): Collateral circulation. *Stroke; a journal of cerebral circulation,*vol.34, no.9, pp.2279-2284.

Li, Q.; Li, J.; Lu, F.; Li, K.; Luo, T.; Xie, P. (2011): A multidetector CT angiography study of variations in the circle of Willis in a Chinese population. *Journal of clinical neuroscience : official journal of the Neurosurgical Society of Australasia,*vol.18, no.3, pp.379-383.

Mantha, A.; Karmonik, C.; Benndorf, G.; Strother, C.; Metcalfe, R. (2006): Hemodynamics in a cerebral artery before and after the formation of an aneurysm. *AJNR. American journal of neuroradiology,*vol.27, no.5, pp.1113-1118.

Meng, H.; Tutino, V.M.; Xiang, J.; Siddiqui, A. (2014): High WSS or low WSS? Complex interactions of hemodynamics with intracranial aneurysm initiation, growth, and rupture: toward a unifying hypothesis. *AJNR. American journal of neuroradiology,* vol.35, no.7, pp.1254-1262.

Moore, S.; David, T.; Chase, J.G.; Arnold, J.; Fink, J. (2006): 3D models of blood flow in the cerebral vasculature. *Journal of biomechanics,*vol.39, no.8, pp.1454-1463.

Nerem, R.M.; Harrison, D.G.; Taylor, W.R.; Alexander, R.W. (1993): Hemodynamics and vascular endothelial biology. *Journal of Cardiovascular Pharmacology,* (21 Suppl 1):S6-10.

Nixon, A.M.; Gunel, M.; Sumpio, B.E. (2010): The critical role of hemodynamics in the development of cerebral vascular disease. *Journal of neurosurgery,*vol.112, no.6, pp. 1240-1253.

Norman, P.E.; Powell, J.T. (2010): Site specificity of aneurysmal disease. *Circulation,*vol.121, no.4, pp.560-568.

Ren, Y.; Chen, G.Z.; Liu, Z.; Cai, Y.; Lu, G.M.; Li, Z.Y. (2016): Reproducibility of image-based computational models of intracranial aneurysm: a comparison between 3D rotational angiography, CT angiography and MR angiography. *Biomedical Engineering Online,* vol.15, no.1, pp.1-14.

Ren, Y.; Chen, Q.; Li, Z.Y. (2015): A 3D numerical study of the collateral capacity of the circle of Willis with anatomical variation in the posterior circulation. *Biomedical engineering online,* (14 Suppl1):S11.

Sadasivan, C.; Fiorella, D.J.; Woo, H.H.; Lieber, B.B. (2013): Physical factors effecting cerebral aneurysm pathophysiology. *Annals of biomedical engineering,* vol.41, no.7, pp. 1347-1365.

Shimogonya, Y.; Ishikawa, T.; Imai, Y.; Matsuki, N.; Yamaguchi, T. (2009): Can temporal fluctuation in spatial wall shear stress gradient initiate a cerebral aneurysm? A proposed novel hemodynamic index, the gradient oscillatory number (GON). *Journal of biomechanics,* vol.42, no.4, pp.550-554.

Tanweer, O.; Wilson, T.A.; Metaxa, E.; Riina, H.A.; Meng, H. (2014): A comparative review of the hemodynamics and pathogenesis of cerebral and abdominal aortic aneurysms: lessons to learn from each other. *Journal of cerebrovascular and endovascular neurosurgery,* vol.16, no.4, pp.335-349.

Zhao, Y.; Chen, B.P.; Miao, H.; Yuan, S.; Li, Y.S.; Hu, Y.; Rocke, D.M.; Chien, S.(2002): Improved significance test for DNA microarray data: temporal effects of shear stress on endothelial genes. *Physiological genomics*, vol.12, no.1, pp.1-11.